



Polyhydroxyalkanoates and biochar from green macroalgal *Ulva* sp. biomass subcritical hydrolysates: Process optimization and a priori economic and greenhouse emissions break-even analysis

Supratim Ghosh^{a,*}, Semion Greiserman^a, Alexander Chemodanov^a, Petronella Margaretha Slegers^b, Bogdan Belgorodsky^c, Michael Epstein^a, Abraham Kribus^d, Michael Gozin^c, Guo-Qiang Chen^e, Alexander Golberg^{a,*}

^a Porter School of the Environment and Earth Sciences, Faculty of Exact Science, Tel Aviv University, Tel Aviv 69978, Israel

^b Operations Research and Logistics, Wageningen University & Research, P.O. Box 8130, 6700 EW Wageningen, the Netherlands.

^c School of Chemistry, Faculty of Exact Science, Tel Aviv University, Tel Aviv 69978, Israel

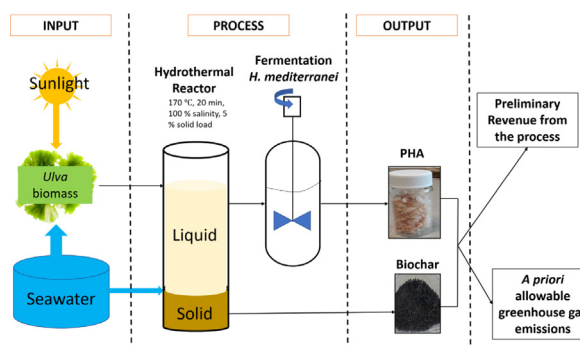
^d School of Mechanical Engineering, Tel Aviv University, Tel Aviv, Israel

^e Center for Synthetic and Systems Biology, School of Life Sciences, Tsinghua University, Beijing, China

HIGHLIGHTS

- Macroalgae as carbon source for PHA production in extreme halophiles.
- Blue economy for sustainable PHA production.
- Preliminary revenue and greenhouse gas analysis.
- Value addition towards a halophilic biorefinery.

GRAPHICAL ABSTRACT



ARTICLE INFO

Article history:

Received 26 November 2020

Received in revised form 14 January 2021

Accepted 16 January 2021

Available online 22 January 2021

Editor: Deyi Hou

Keywords:

Biochar

Haloferax mediterranei

Polyhydroxyalkanoates

Subcritical hydrolysate

Ulva sp.

ABSTRACT

Although macroalgae biomass is an emerging sustainable feedstock for biorefineries, the optimum process parameters for their hydrolysis and fermentation are still not known. In the present study, the simultaneous production of polyhydroxyalkanoates (PHA) and biochar from green macroalgae *Ulva* sp. is examined, applying subcritical water hydrolysis and *Haloferax mediterranei* fermentation. First, the effects of temperature, treatment time, salinity, and solid load on the biomass and PHA productivity were optimized following the Taguchi method. Hydrolysis at 170 °C, 20 min residence time, 38 g L⁻¹ salinity with a seaweed solid load of 5% led to the maximum PHA yield of 0.104 g g⁻¹ *Ulva* and a biochar yield of 0.194 ± 1.23 g g⁻¹ *Ulva*. Second, the effect of different initial culture densities on the biomass and PHA productivity was studied. An initial culture density of 50 g L⁻¹ led to the maximum volumetric PHA productivity of 0.024 ± 0.002 g L⁻¹ h⁻¹ with a maximum PHA content of 49.38 ± 0.3% w/w. Sensitivity analysis shows that within 90% confidence, the annual PHA production from *Ulva* sp. is 148.14 g PHA m⁻² year⁻¹ with an annual biochar production of 42.6 g m⁻² year⁻¹. Priori economic and greenhouse gas break-even analyses of the process were done to estimate annual revenues and allowable greenhouse gas emissions. The study illustrates that PHA production from seaweed hydrolysate using extreme halophiles coupled to biochar production could become a benign and promising step in a marine biorefinery.

© 2021 Elsevier B.V. All rights reserved.

* Corresponding authors at: Porter School of the Environment and Earth Sciences, Faculty of Exact Science, Tel Aviv University, Tel Aviv 69978, Israel.
E-mail address: supratim4737@gmail.com (S. Ghosh).

1. Introduction

Macroalgae or seaweeds are a sustainable and renewable resource because of their various advantages over conventional sources of biomass. Seaweed cultivation does not require freshwater and arable land and thus does not compete with food crops (Gao et al., 2020). Moreover, it does not contain lignin which is important for biomass processing (Greiserman et al., 2019). Lignin is associated with cellulose in plant cell walls which hinders the availability of cell wall polysaccharides to enzymatic treatment to smaller utilizable monosaccharides which is not the case for macroalgae (Xu et al., 2020; Yu et al., 2020). Almost all components of macroalgal biomass are directly utilized for various purposes in the food, biotechnology, pharma, and energy sectors. For example, macroalgae contain unique polysaccharides such as ulvan, carrageenan, alginate, mannitol, and agar that have therapeutic and industrial usages (Prabhu et al., 2020). Besides, macroalgal biomass can be converted to several products through thermochemical and biological pathways (Golberg et al., 2020). For example, the sugars present in macroalgal biomass can be fermented to biofuels such as bioethanol (Polikovskiy et al., 2020) or biomethane (Gao et al., 2020) and polymers such as polyhydroxyalkanoates (PHA). One of the key steps for seaweed biomass fermentation includes the fragmentation of complex carbohydrates into their fermentable ingredients. Also, fermentability and PHA yield depend on the composition of the hydrolysates, which is not well defined but depends on the processing conditions (Greiserman et al., 2019).

There are various methods for pre-treatment of seaweed biomass. These include mechanical (Korzen et al., 2015), thermal (Jayakody et al., 2018), chemical hydrolysis (Pezoa-Conte et al., 2015), electrochemical (Robin et al., 2018), enzymatic hydrolysis (Qarri and Israel, 2020), or a combination of various pretreatment methods (Thompson et al., 2019). Although these methods have been proven to be effective in the conversion of macroalgal complex carbohydrates, they either require high energy or cost inputs and the chemical outputs from the processes are toxic to the environment. An alternative and sustainable solution to the problem could be the subcritical hydrolysis of macroalgal biomass (Greiserman et al., 2019).

Subcritical hydrolysis as an outcome of hydrothermal carbonization (HTC) could be used to process macroalgal biomass by converting the complex polysaccharides of the seaweed into fermentable sugars. Reaction temperatures of 180 °C could be enough for efficient conversion of the seaweed biomass to fermentable sugars. The hydrolysates could be utilized in various fermentation processes to produce biofuels such as bioethanol and biohydrogen. It can also be utilized to produce various other bioproducts which include lipids and polyhydroxyalkanoates (PHAs). The other major product in the subcritical hydrolysis of biomass is biochar. Numerous studies have been reported about converting biomass and biomass waste into biochar and in recent years studies have been performed also with macroalgae (Brown et al., 2020; Yoganandham et al., 2020). Some recent studies have also focused on the co-production of biochar and sugars for further fermentation to biofuels and bioproducts (Greetham et al., 2020).

Although the use of PHA for the replacement of fossil-derived polyesters has been proposed decades ago, the penetration of PHA to the plastic market is slow due to their cost. The key parameter in the cost of the final PHA is the economic and environmental cost of the feedstock and the conversion yield of the initial biomass to PHA. For seaweeds, the conversion yields by *Halofexax mediterranei*, which depend on both hydrolysis and fermentation parameters, have not been optimized yet. Our previous study on PHA production by *Halofexax mediterranei* using *Ulva* sp. biomass hydrolysates provided an insight into the process which led to a method that was devoid of freshwater usage, thereby indicating a feasible process scale-up (Ghosh et al., 2019). Various process parameters such as the temperature of the reaction, solid load, and the duration of hydrolysis determine the composition of hydrolysate and the extent of PHA produced after fermentation (Greiserman et al., 2019). Notably,

the effect of these process parameters on the PHA yield from *Ulva* biomass has not been explored yet. Besides, the co-production strategy of the simultaneous production of biochar and PHA has not been explored. Such a pathway could further reduce the direct costs and waste from seaweed to PHA fermentation.

The goal of this study is to address these key challenges and define the effect of hydrolysis and fermentation parameters' impact on the green macroalgae *Ulva* sp. biomass conversion to PHA with *H. mediterranei*. This is an important next step required to bring sustainable PHA to broad industrial adaptation. Among macroalgal species, *Ulva* sp. is one of the most versatile because of its high growth rates, availability, and costs (Golberg et al., 2020). Reports have been published on green tides due to *Ulva* sp. which are the main cause of eutrophication and are thus an environmental problem (Cui et al., 2018). To collect bloom-forming algae for biofuels and bioproducts is not only waste reuse but only can reduce the cost because cultivation accounts for a large proportion of the total cost (Gao et al., 2019, 2018). So, the hydrothermal processing of *Ulva* sp. provides a simultaneous strategy of waste remediation and value-added product generation. In this work, the process conditions, including temperature, residence time, solid load, and salinity were improved by the Taguchi orthogonal array design for efficient PHA production from the hydrolysate. Also, the effect of different initial culture densities on the biomass and PHA productivity was studied. Various analytical methods were employed to determine the structural characteristics of PHA. Based on the experimental data, a preliminary revenue analysis of PHA production from seaweed hydrolysate was statistically estimated keeping in mind the seasonal variations of seaweed and PHA production in Israel. Based on these data, we evaluated a priori the economic potential and allowable greenhouse gas emissions of the production chain. The proposed co-production could provide an additional advantage to the subcritical hydrolysis of macroalgal biomass. This, in turn, could be a renewable and sustainable process for PHA production in the long run.

2. Materials and methods

2.1. Macroalgal biomass production

The macroalgae under investigation in the present study belonged to the genus *Ulva* (taxonomic status of this seaweed is under investigation). The seaweed was collected from the shallow waters and intertidal areas of the Israeli Mediterranean coast. Cultivation of *Ulva* sp. was performed in custom-made outdoor photobioreactors (Polytiv, Israel). The photobioreactors had dimensions of 100 cm in length, a width of 40 cm with a thickness of 200 mm. Sunlight was utilized for the growth of macroalgal biomass which led to varied productivities throughout the year depending on the natural irradiance. The cultivation conditions were according to our previous study (Chemodanov et al., 2017). The seaweed was cultivated in artificial seawater (ASW) cultivation medium which was prepared using distilled water containing dissolved dried Red Sea Salt (Red Sea Inc., IS) which had a total salinity of 37‰. Ammonium nitrate (NH_4NO_3 , Haifa Chemicals Ltd., IS) and phosphoric acid (H_3PO_4 , Haifa Chemicals Ltd., IS) were added to the ASW medium to maintain a concentration of 6.4 g m^{-3} of nitrogen (N_2) and 0.97 g m^{-3} of phosphorus (P) respectively. The initial inoculum of seaweed was 20 g of *Ulva* sp. in the 40.4 L photobioreactor. Other parameters such as pH, temperature, and airflow rate were maintained according to our previous study (Chemodanov et al., 2017).

2.2. Subcritical thermal hydrolysis experimental setup

Subcritical thermal hydrolysis was achieved in a batch reactor (0.25 L) as shown in Fig. 1a. The heating was performed using an electric heater (CJF-0.25, Keda Machinery, China). The temperature inside the reactor was measured using a digital temperature gauge (MRC TM-5005) equipped with a K-type thermocouple (Watlow, USA). The



Fig. 1. (a) Dried *Ulva* biomass used for hydrolysis. (b) Experimental setup for PHA production using hydrolysate. (c) PHA obtained after extraction. (d) Digital image of *Ulva* biochar after hydrolysis. (e) Experimental setup for hydrolysis of *Ulva* biomass. 1. Electric heater 2. Reactor 3. Stirrer motor 4. Heat exchanger 5. Pressure sensor 6. Thermocouple 7. Temperature gauge 8. Pressure gauge 9. Controller.

pressure inside the reactor was measured using a pressure gauge and sensor (MRC PS-9302, MRC PS100-50 bar). To facilitate mixing inside the reactor, it was equipped with a stirrer with water cooling. Sampling ports for liquid and gas sampling were present in the reactor. The sampling ports were connected to individual condensers and cooling traps for efficient sampling. Cooling of the reactor was done using an industrial chiller (S&A, Guangzhou, China). Before every experiment, the air was evacuated from the reactor using a vacuum pump (MRC ST-85).

2.3. Optimization of subcritical hydrolysis for PHA production using Taguchi method

The effect of various process parameters (temperature, pre-treatment time, salinity, and solid load) for thermal hydrolysis on the PHA production process was estimated using the Taguchi method. The Taguchi method was employed to decrease the number of experiments to determine the impact of each parameter independently. Various studies have been conducted and the efficacy of optimization using the Taguchi approach has been tested (Rao et al., 2008).

The impact of the following range of HTC parameters was tested, using the L9 Taguchi matrix: temperature of 170, 187, 205 °C; Solid load of 2, 5, 8%; Residence time of 20, 40, 60 min; and Salinity of 0, 19, 38 g L⁻¹. The L9 orthogonal experimental array for the determination of individual effects of process parameters on PHA production is provided in Table 1. The experiments were repeated in triplicate and the best target function was investigated using analytical software (Minitab Inc., USA). The experimental design (Taguchi) utilizes a signal-to-noise ratio (SN) to determine the most effective parameter for the process.

The present study used “the larger the better” algorithm for efficient design methodology. The SN ratio was calculated according to Eq. (1):

$$SN^{OUT_max}(j) = -10 \cdot \log \left[\frac{1}{\#R} \sum_{R=1}^{\#R} \frac{1}{(m_{rep})^2} \right] \quad 1 \leq j \leq K \quad (1)$$

in which the experiment number is denoted by K, the repetitions of experiments is represented by #R, and the outcome for a precise repetition R for any experiment j is symbolized by m_{rep} .

The average SN ratio for each process parameter P with a level V was determined according to Eq. (2):

$$SN^{OUT}(P, V) = \frac{1}{n(P, V)} \sum_{j \in \{P, V\}} SN^{OUT} \quad (2)$$

For determination of the most effective parameter of the process, a sensitivity (Δ) value for each parameter was calculated using Eq. (3):

$$\Delta^{OUT}(P) = \text{Max}\{SN^{OUT}(P, V)\} - \text{Min}\{SN^{OUT}(P, V)\} \quad (3)$$

According to values obtained for sensitivity analysis, a rank (1–4, with 1 being the largest rank) was given to the parameters under investigation.

2.4. PHA production by *H. mediterranei* using seaweed hydrolysate

Following hydrolysis, the liquid phase (hydrolysate) was utilized as a substrate for fermentation using *Haloferax mediterranei* ATCC 33500

Table 1
Design of experiment using L9 Taguchi matrix.

Experiment no.	Temperature (°C)	Solid load (% dry algae weight/total mixture weight)	Residence time (min)	Salinity (% sea water) 100% = 38gsalt L ⁻¹
1	170	2	20	0
2	170	5	40	50
3	170	8	60	100
4	187	2	40	100
5	187	5	60	0
6	187	8	20	50
7	205	2	60	50
8	205	5	20	100
9	205	8	40	0

(NCIMB 2177) as a fermentative organism. The seaweed hydrolysates for PHA production were used at a concentration of 25% v/v of medium as observed in previous studies (Ghosh et al., 2019). The salinity of the medium was adjusted to the Hv-YPC medium (25% w/v) (Allers et al., 2010) and peptone was utilized as the nitrogen source. The experiments were performed in 100 mL bottles (Schott Duran, USA) with 50 mL working volume (Fig. 1b). The initial pH of the medium was adjusted to pH 7.2. The fermentation was performed at 42 °C in a temperature-controlled shaking incubator at 100 rpm (Benchmark Scientific, USA).

2.5. PHA extraction

The fermentation broth was collected and centrifugation was performed at 10000 rpm for 10 min (Yingtai Instruments TGL-18, China). The cell pellet after centrifugation was dried at 60 °C for a period of 12 h in a convection oven (MRC Labs, Israel). The dry cell weight of the biomass was determined. To the cell pellet, 100 ml of distilled water with 0.1% sodium dodecyl sulphate (SDS) was added and was kept for 24 h. After lysis, the cell suspension was transferred to a fresh tube and was centrifuged at 9000 rpm for 15 min to separate the pellet from the supernatant. The process was repeated until a white-colored pellet was obtained. The pellet was then dried to a constant weight in a hot air oven (Ex-Lab Scientific, IS) at 40 °C and further analysis was conducted.

2.6. Quantification of intracellular PHA content

Intracellular PHA content of *H. mediterranei* was measured using the Nile Red Staining procedure according to Spiekermann et al. (1999) (Spiekermann et al., 1999). The cells were washed with 10% saline and resuspended. The Nile Red (Sigma, USA) concentration was adjusted to 3.1 µg mL⁻¹. After an incubation time of 30 min, the cell pellet was washed with 10% saline and resuspended. A standard curve was plotted by analyzing the fluorescence at excitation and emission wavelengths of 535 and 605 nm respectively in a spectrofluorometer equipped with a 96-well microtiter plate reader (Tecan, Switzerland). The quantifications were performed in triplicate for each measured value. Further verification of the PHA quantity was performed using the crotonic acid assay (Mahansaria et al., 2018).

2.7. Determination of volumetric biomass and PHA productivity

The calculation for biomass productivity was performed using Eq. (4):

$$X_B = \frac{B_2 - B_1}{t_2 - t_1} \quad (4)$$

in which X_B denotes the volumetric biomass productivity in units of g L⁻¹ h⁻¹, B_1 is the biomass concentration at time t_1 and B_2 is the biomass concentration at time t_2 .

Furthermore, the volumetric PHA productivity was calculated according to Eq. (5):

$$X_P = \frac{C_2 - C_1}{t_2 - t_1} \quad (5)$$

where X_P signifies the volumetric PHA productivity in g L⁻¹ h⁻¹, C_1 is the PHA content at time t_1 and C_2 is the PHA content at time t_2 .

The yield of PHA (% w/w) was calculated according to Eq. (6):

$$\text{Yield} = \frac{W_{\text{PHA}}}{W_{\text{cell}}} \times 100 \quad (6)$$

in which W_{PHA} (g) is the quantity of PHA obtained from dry cell weight of biomass (W_{cell} , g).

2.8. Characterization of PHA

2.8.1. FTIR analysis

FTIR spectra of air-dried PHA films (Fig. 1d) were measured on a spectrometer equipped with Attenuated Total Reflectance attachment (Bruker Platinum ATR) in a spectral range of 400 to 4000 cm⁻¹.

2.8.2. TGA/DSC analysis

Differential scanning calorimetry with simultaneous thermogravimetry (DSC-TG) analyses was carried out on a system equipped with an autoloader (Jupiter STA 449 F5, NETZSCH, Germany). In a typical analysis, a dry sample of PHA biopolymer (5 mg) was placed into a sealed aluminum pan and subjected to a linear temperature increase in a range from 30 to 600 °C, with a heating rate of 10 °C · min⁻¹.

2.8.3. ¹H NMR analysis

¹H NMR spectra were measured by dissolving the PHA samples in deuterated chloroform (CDCl₃), at concentration of 10 mg · mL⁻¹ and analyzed on a 400 MHz spectrometer (Bruker, USA).

2.9. GC/MS analysis

2.9.1. GC/MS analysis of seaweed hydrolysate

0.6 ml of sample extracted with two aliquots of dichloromethane (DCM) (0.3 ml) were combined and analyzed. The analysis was performed in a Gas Chromatograph (GC) equipped with a mass spectrometer (MS) analyzer (Agilent, USA). The column used for separation was a (5% phenyl)-methylpolysiloxane column with dimensions of 30 m in length and an internal diameter of 0.25 mm (Agilent, USA). The details of the method for GC analysis were according to our previous publication (Steinbruch et al., 2020).

2.9.2. GC/MS analysis of PHA produced

The PHA obtained after extraction was further analyzed using GC/MS. The PHA was modified for analysis according to the procedure as provided in our earlier work (Ghosh et al., 2019). The liquid phase was analyzed using GC equipped with an MS detector (Agilent, USA). The detailed method for GC analysis was similar to our previously published work (Ghosh et al., 2019).

2.10. Molecular weight analysis

The PHA samples were analyzed by Gel Permeation Chromatography (GPC) (by TAMI-IMI Ltd. analytical laboratory, Israel) to determine the molecular weights distributions of PHA polymers vs Polystyrene Standards and Poly (methyl methacrylate) standards. The samples were extracted by chloroform and analyzed by GPC. The columns used were Phenomenex, Security Guard column GPC 4 * 3 mm, and Phenomenex, Phenogel, Columns 300 * 7.8 mm * 5 μm (Phenomenex, USA). The flow rate of the mobile phase Tetrahydrofuran (THF) was maintained at 1 mL min⁻¹ with a sample injection amount of 10 μL at 40 °C.

2.11. Biochar and water-soluble solid mass recovery

Fig. 1d shows the dried *Ulva* biomass which was utilized for biochar formation. The obtained biochar is shown in Fig. 1e. At the end of each experiment, a liquid sample was taken and dried for calculation of the water-soluble solids. The residue (solid and liquid) was dried at 40 °C. The biochar yield was then calculated by subtracting the water-soluble solids (which were calculated by multiplying the amount of solid left from the dried liquid sample by the quotient of the total liquid dried in the residue and the liquid sample taken) from the total solid left after drying.

2.12. Potential revenue estimation from PHA and biochar production from offshore grown *Ulva* sp. biomass

The sugar compositions of *Ulva* sp. vary with changes in environmental conditions as well as other external factors involved in offshore cultivation. This affects PHA productivity. To estimate the potential revenue from PHA production using *Ulva* sp. as a substrate, variation in the cultivation yields throughout the year, as measured by us before, was considered (Chemodanov et al., 2017). Based on this metadata, the conversion efficiency of seaweed biomass to PHA was estimated using a probability density function denoted as conversion efficiency distribution (CED). This was based on the year-long cultivation data – each data (yield per g substrate) gets equal weight. The CED is expressed as $[g_{PHA} g^{-1} DW_{Ulva}]$:

$$CED \left[\frac{g_{PHA}}{g_{Ulva}} \right] = \frac{m_{PHA} [g_{PHA}]}{m_{UlvaDW} [gDW_{Ulva}]} \quad (7)$$

For a cultivation interval amid two subsequent fermentations $d = 1 \dots x$, in which x is the quantity of fermentations achieved annually ($x = 80$ in this scenario, assuming that fermentation is performed every time the seaweeds are harvested), let $PPR(d)$ represent the arbitrary variable that designates the PHA Production Rate through the cultivation interval amid two consecutive intervals. Due to fluctuations in the annual biomass yield (DGR), to achieve the distribution of $PPR(d)$, the static distribution of the conversion rate was multiplied by the annual growth rate (DGR) calculated like former studies (Chemodanov et al., 2017) as follows:

$$PPR(d) [g_{PHA} m^{-2} d^{-1}] = DGR [gWW_{Ulva} m^{-2} d^{-1}] \cdot \frac{DW_{Ulva}}{WW_{Ulva}} \cdot CED \left[\frac{g_{PHA}}{g_{Ulva}} \right] \quad (8)$$

The annual PHA production is the summation of manufacture yields at the cultivation durations: $d = 1 \dots x$. So, the annual PHA production rate ($APPR$) is computed according to Eq. (9):

$$APPR [g_{PHA} m^{-2} year^{-1}] = \sum_{d=1}^n PPR(d) \quad (9)$$

Between any two stages of fermentation, it is assumed that they are independent of each other. Therefore, the distribution of $APPR$ can be estimated by recurrent convolution of $PPR(d)$. This was calculated by a custom-made script developed in R (RStudio Inc., USA).

The distribution of the maximum admissible price of *Ulva* sp. biomass for PHA production was calculated according to Eq. (10):

$$C [\$ \cdot ton^{-1}] = P_{PHA} [\$ \cdot kg^{-1}] \cdot CED \cdot f \quad (10)$$

in which C ($\$ \cdot ton^{-1}$) is the admissible price of the biomass, P_{PHA} ($\$ \cdot kg^{-1}$) denotes the present cost of PHA ($\$4$ – $\$10 \cdot kg^{-1}$) (Vandit et al., 2018), CED is PHA conversion efficiency, and f denotes the portion allotted for PHA production in the total costs accountable to biomass production. The current price of PHA is known and is not competitive with regular fossil fuel-based plastics. The goal is to find a point when they will be. In the present study, we calculated the maximum possible cost of *Ulva* sp. biomass which could be feasible using the current market price of PHA. This information is essential because, to make the process profitable enough, the minimum price of the substrate should be determined. This in turn could be utilized for further decreasing the final price of the product.

2.13. Estimation of allowable greenhouse gas emissions

In this work, the a priori maximum allowable GHG emissions of macroalgae cultivation and processing into PHA (excluding use and end-of-life) are determined by downscaling the current GHG emissions of alternative PHA production to seaweed PHA production. To estimate the distribution of the maximum allowable greenhouse gas (GHG) emissions of the biomass for PHA production the following Eq. (11) was applied:

$$E_{DW_{biomass}} \left[\frac{ton \ CO_2}{ton} \right] = E_{PHA} \left[\frac{kg \ CO_2}{kg} \right] \cdot CED \cdot f \quad (11)$$

where $E_{DW_{biomass}}$ ($ton \ CO_2$ -equivalent ton^{-1}) is the maximum allowable GHG emissions from the *Ulva* sp. biomass, E_{PHA} (CO_2 -equivalent kg^{-1}) are the current GHG emissions of PHA (see supplementary material for the evaluated scenarios), CED is denoted as Eq. (6) in the previous section, and f is the fraction of the total GHG emissions of PHA production accountable to biomass production. The evaluated current GHG emissions of alternative PHA production E_{PHA} are fossil-based High-Density Polyethylene (HDPE) and state-of-the-art biobased PHA production from wastewater, sugar crops, and oil crops. Feedstock production is assumed to account for 35% of the emissions of PHA, similar to alternative biobased PHA production systems (Akiyama et al., 2003).

2.14. Statistical analysis

In order to avoid variability in the results, the experiments were performed in triplicate. Standard deviation (SD) was calculated from the mean of the three values. The final values were represented as mean \pm SD. The Taguchi analysis was performed using the Minitab software (Minitab, USA). The graphs were plotted using the Sigmaplot software (Sigmaplot, USA).

3. Results and discussion

3.1. Effect of optimized hydrolysate production conditions (Taguchi) on the PHA productivity

The effect of hydrolysis parameters on the PHA yield was studied using seaweed hydrolysate as a substrate. The Taguchi orthogonal array analysis suggested that temperature had the highest impact on the PHA yield (Rank 1) followed by the salinity of the medium (Rank 2) and residence time (Rank 3). The analysis also suggested that solid load has a very small or no effect on the PHA production process (Rank 4). The analysis along with the ranks and sensitivity (Δ) values is shown in Table 2. Temperature plays an important role in the production of monosaccharides for use in fermentation to produce PHA. Higher temperatures would lead to the production of inhibitory substances such as 5-hydroxymethyl furfural (5-HMF) which in turn could be toxic for the fermentative organism. Similar observations were reported by Greiserman et al., 2019 where they elucidated the consequence of different hydrolysis factors on the sugar content of *Ulva* hydrolysates (Greiserman et al., 2019). Also, the rates of heating and cooling determine the extent of chemical reactions in subcritical hydrolysis which can determine the various products obtained from hydrothermal carbonization. Higher temperatures of hydrothermal carbonization could lead to isomerization of the monosaccharides produced. This in turn could affect the PHA fermentation process thereby decreasing the PHA yield due to the non-availability of the sugars. The temperature is an important factor that determines the quantity and quality of monosaccharides produced which can be utilized in the fermentation process. The Taguchi analysis also suggests that temperature is the most important factor governing the PHA production process. Therefore, controlling the temperature of hydrolysis could lead to higher PHA yields. Higher temperatures may lead to higher energy and cost inputs which might be harmful to the overall process. Similarly, lower temperatures of hydrolysis may lead to lower yields of reducing sugars thereby reducing the amount of PHA produced. Moreover, complex system needs for the process may lead to difficulties in scaleup of the process. So, it becomes imperative to optimize the process parameters which have been shown in the present study. Salinity plays an important role in the hydrothermal processing of biomass. The studies by Jones et al., 2020 showed that saline water helped in the catalysis reaction of the biomass which in turn increased the aqueous and biochar yields of the HTL process. The presence of saline water was beneficial as compared to conventional distilled water used for hydrothermal processing of macroalgal biomass (Jones et al., 2020). Similar studies on the effect of salinity were observed by Greiserman et al., 2019 where they found that salinity was an important factor for the release of monosaccharides from macroalgal biomass using hydrothermal pre-treatment (Greiserman et al., 2019).

The sensitivity of PHA production using hydrolysates to the established factors was evaluated (Fig. 2). The temperature of the hydrolysis suggestively affected the PHA production process (Fig. 2a). Taguchi method utilizes the signal to noise (S/N) ratio to determine the variation in the experiment due to uncontrollable parameters. The

experimental control factors fall under the “signal” regime while the “noise” is the variation due to the experimental factors. This method helps in reducing variability in the experiment by using larger the better S/N ratio thereby avoiding the loss of function in the overall experiment (Venkata Mohan and Venkateswar Reddy, 2013). A greater S/N ratio indicates the better performance of that parameter towards PHA production. Higher values of S/N ratio identify control factors that minimize the effect of noise factors. According to the S/N ratio values, the delta values were calculated and corresponding ranks were given to the factors which determine their effect on the PHA production process. The S/N ratio of different factors indicated that temperature and salinity play an important part in PHA production. Therefore, controlling the temperature may lead to an increase in PHA yield using seaweed hydrolysate as a substrate. Fig. 2b shows the interaction plots between the process parameters under study. The significance of interaction is assumed by the line plots. If they run parallelly, it suggests that there is no interaction between the process parameters under observation. The intersection between plots denotes interaction. The plots between temperature and salinity suggest that interactions between factors were observed at certain levels. At a salinity of 19 g L⁻¹ and 38 g L⁻¹, no interaction was observed between temperature and salinity but the factors interacted at a salinity of 0 g L⁻¹. Temperature and salinity showed no interactions as no intersection was observed between the two factors. This has future implications for scale-up of the process where temperature and salinity play a major role as discussed in the previous section. An interaction between salinity and the solid load was observed at lower salinities but was not observed at higher salinities. This might be since, at higher salinities, the salt content of the macroalgal biomass becomes insignificant as compared to lower salinities which might affect the hydrolysis process. Recent studies on PHA production under high salinity conditions have established that three pathways are affected as a response to hypertonic pressure. Two proteins, namely, beta-ketoacyl-ACP reductase and 3-hydroxyacyl-CoA dehydrogenase, were overexpressed resulting in the higher production of PHA. The serine-pyruvate transaminase and serine-glyoxylate transaminase were upregulated, thereby increasing the conversion of glucose to PHA. Some proteins such as sulphate-adenyl transferase and adenylyl-sulphate kinase were downregulated resulting in a decrease in PHA synthesis (Pacholak et al., 2020). Using the Taguchi Design of Experiment, the optimum parameters for the maximum PHA production (the maximum SN ratio) were determined as 170 °C, 20 min residence time, 38 g L⁻¹ salinity with a solid load of 5%.

The macroalgal hydrolysates obtained were used for PHA production by *Haloferax mediterranei*. The profiles for biomass concentration, PHA content, and PHA yield are provided in Fig. 3. Macroalgal hydrolysate no. 3 yielded the highest biomass and PHA yield. The final biomass concentration after a fermentation interval of 120 h was observed to be 3.9 ± 0.25 g L⁻¹. These values correspond to a maximum internal PHA concentration of 2.08 ± 0.34 g L⁻¹. PHA content of the biomass was also calculated which amounted to 53% w/w of the biomass obtained. Volumetric productivities amounted to a maximum of 0.0325 ± 0.008 g L⁻¹ h⁻¹ and 0.017 ± 0.002 g L⁻¹ h⁻¹ for biomass and PHA respectively. The yield was also calculated per gram of macroalgae. Therefore, 1 g of algae yielded approximately 0.104 g of PHA for a single batch fermentation. Several studies have reported similar biomass and PHA productivities (0.002–0.900 g L⁻¹ h⁻¹). Laboratory scale studies (100–250 mL of reactor working volume) might be the probable cause for the ranges of volumetric PHA productivities using macroalgal hydrolysates as a substrate. The process parameters in a bioreactor should be further optimized to achieve improved efficiencies (Cesário et al., 2018). This has been demonstrated by various studies where the statistical optimization of process parameters in a bioreactor leads to higher PHA productivities. Arumugam et al., 2020 optimized the process parameters (concentrations of carbon, nitrogen, and inoculum) using Response Surface Methodology (RSM) to enhance the PHA productivity of *Cupriavidus necator* using non-edible oils as a substrate (Arumugam

Table 2

Response table for signal to noise ratios and ranking of hydrolysis parameters using the Taguchi approach.

Level	Temperature (°C)	Solid Load (%)	Residence Time (min)	Salinity (g L ⁻¹)
1	32.40	27.24	29.54	26.43
2	31.93	29.03	28.05	27.09
3	19.86	27.92	26.60	30.67
Sensitivity (Δ)	12.54	1.78	2.94	4.23
Rank	1	4	3	2

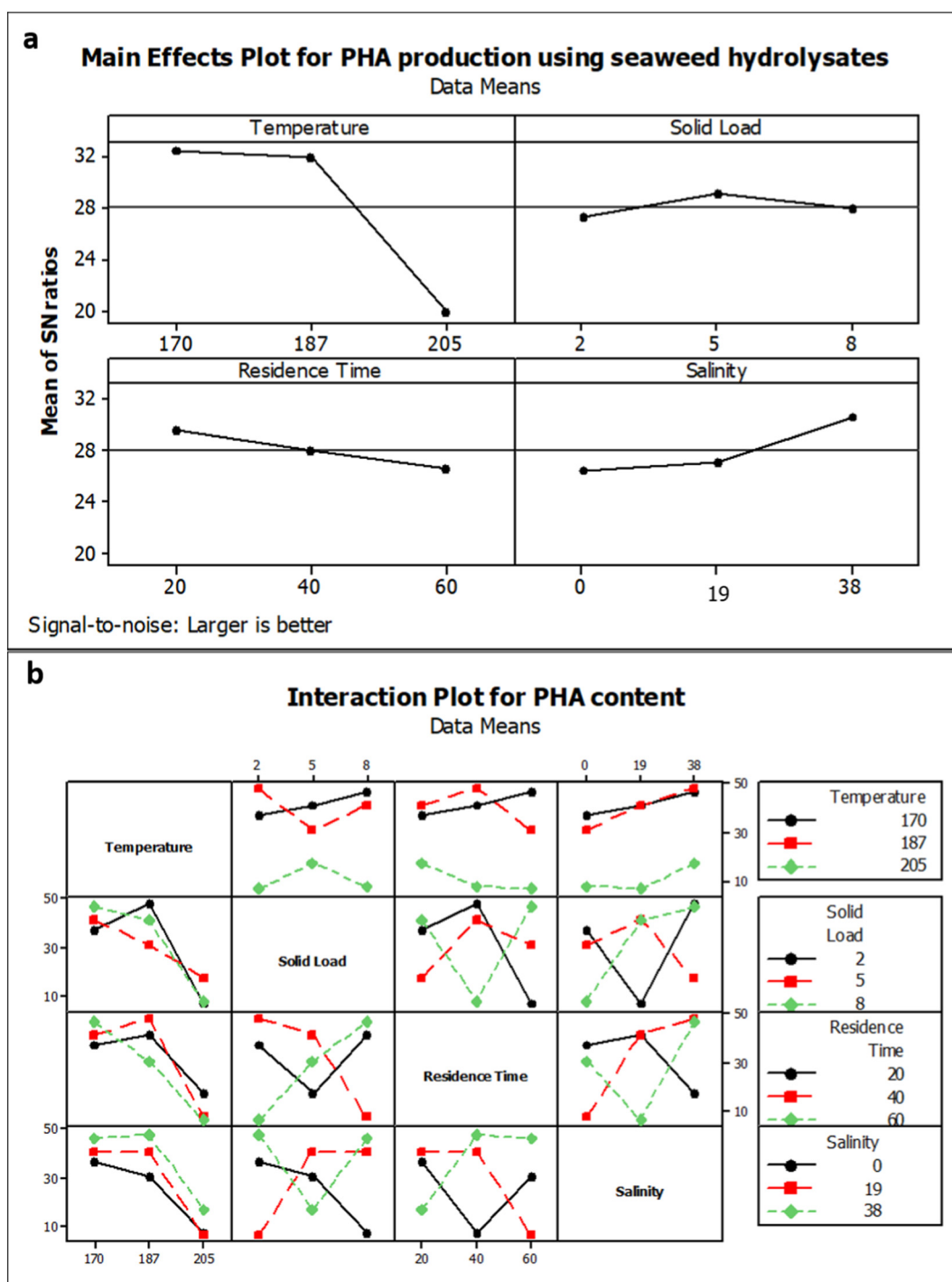


Fig. 2. (a) Taguchi analysis of the impact of 4 HTC parameters on the PHA production utilizing macroalgal hydrolysates as substrate. The effects of HTC parameters such as Temperature ($^{\circ}\text{C}$), Solid load (%), Residence time (min), and Salinity (g L^{-1}) were tested. (b) Interaction plots for the effect of different factors on the PHA production using seaweed hydrolysate as a substrate.

et al., 2020). RSM was also utilized by Mohd Zain et al. (2020) where they enhanced the PHA productivity of *Burkholderia cepacia* BPT1213 using waste glycerol from the biodiesel industry as a substrate. They optimized the aeration rate, agitation speed, and cultivation time in a batch bioreactor (Mohd Zain et al., 2020).

3.2. Effect of initial culture density on the volumetric PHA productivity

The studies were performed using initial culture densities in the range of $10\text{--}500 \text{ g L}^{-1}$ in standard cultivation media and seaweed

hydrolysate medium. Using standard cultivation media, the maximum biomass concentration of $57.57 \pm 0.033 \text{ g L}^{-1}$ with a maximum PHA content of $53.58 \pm 0.12\% \text{ w/w}$ was obtained at an initial culture density of 50 g L^{-1} . Similarly, using a seaweed hydrolysate medium, the maximum biomass concentration obtained was $56.02 \pm 0.24 \text{ g L}^{-1}$ with a maximum PHA content of $49.38 \pm 0.3\% \text{ w/w}$ at an initial culture density of 50 g L^{-1} . At higher concentrations (beyond 100 g L^{-1}), no significant growth was observed. During the growth of a microorganism, end products accumulate in the medium to such an extent that the metabolic activity is suppressed (Luong

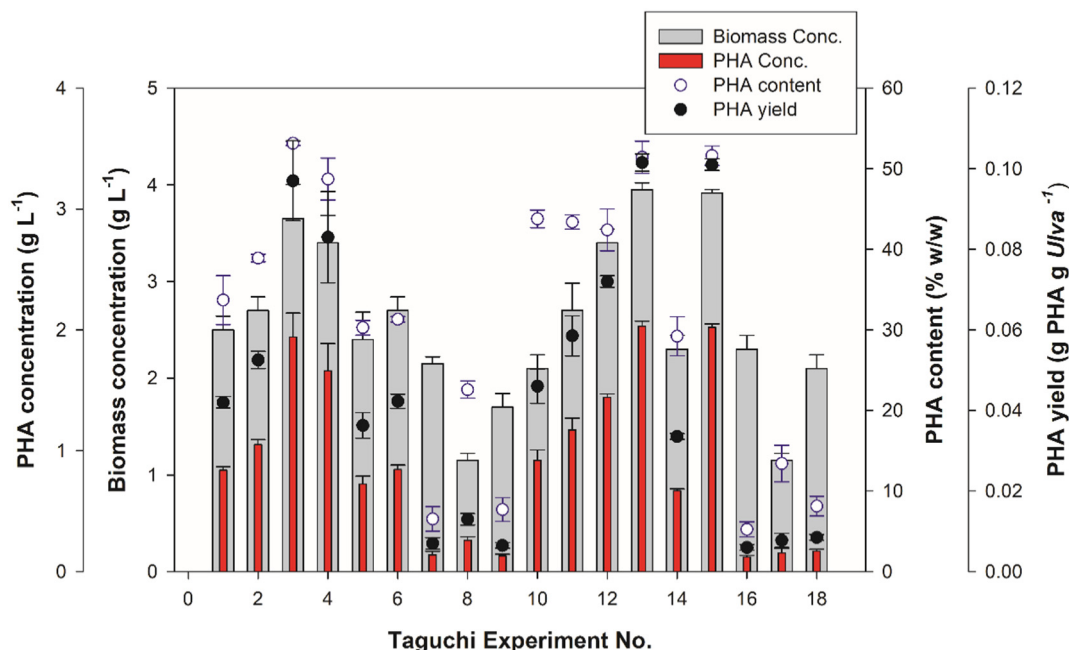


Fig. 3. Biomass concentration, PHA concentration, and PHA content and PHA yields for *Haloferax mediterranei* cultivated on macroalgal hydrolysates.

and Mulchandani, 1989). This might be the probable reason for lower growth at higher initial culture density. The productivities were also calculated for various culture densities. The maximum biomass productivity of $0.0631 \pm 0.0002 \text{ g L}^{-1} \text{ h}^{-1}$ with a PHA productivity of $0.033 \pm 0.0002 \text{ g L}^{-1} \text{ h}^{-1}$ was obtained at an initial culture density of 50 g L^{-1} using standard Hv-YPC medium. Similarly, using a seaweed hydrolysate medium, maximum biomass productivity of $0.05 \pm 0.002 \text{ g L}^{-1} \text{ h}^{-1}$ with a maximum PHA productivity of $0.024 \pm 0.002 \text{ g L}^{-1} \text{ h}^{-1}$ was obtained at an initial culture density of 50 g L^{-1} . Similar results were obtained by Ibrahim and Steinbüchel, 2009, where they obtained high PHA yields ($\sim 66\% \text{ w/w}$) at higher culture densities ($55\text{--}85 \text{ g L}^{-1}$). They utilized *Zobellella denitrificans* MW1 as PHA producing an organism with glycerol as a substrate (Ibrahim and Steinbüchel, 2009). Another study showed that PHA can be produced using waste cooking oil by *Pseudomonas putida* KT2440 at high cell densities of 154.9 g L^{-1} with a PHA content of $34\% \text{ w/w}$ (Ruiz et al., 2013). Studies by Hori et al., 2019 showed a high-cell density culture of poly(lactate-co-3-hydroxybutyrate)-producing *Escherichia coli* with similar results (Hori et al., 2019). A study by Alsafadi et al., 2020 utilized date palm waste for PHA production by *H. mediterranei*. They obtained a final PHA content of $25\% \text{ w/w}$ under fed batch cultivation conditions (Alsafadi et al., 2020). Another study by Abdallah et al., 2020 utilized inexpensive substrates for PHA production by haloarchaeal isolates. They reported a final PHA concentration of $35\% \text{ w/w}$ under optimized cultivation conditions (Abdallah et al., 2020). Advantages of high-cell density cultivation systems include increased productivity along with reduced costs of downstream processes and wastewater treatment. High cell density cultivations demand a higher oxygen mass transfer which in turn limits the flow of substrate to the bulk culture medium. This has to be kept in mind while designing a system with high cell density cultivation. Also, for reducing the costs of PHA production, pure oxygen must be avoided for aeration of the culture. Dissolved oxygen (DO) concentration is a key parameter for the development of high-cell-density cultivation of obligate aerobic microorganisms. High O_2 demand and increasing difficulty for O_2 transport and dispersion owing to modification of the physical properties of the fermentation broth (mainly viscosity and surface tension) limit the final cell concentration.

3.3. Structural analysis of PHA produced (FTIR, TGA/DSC, ¹H NMR)

3.3.1. FTIR analysis

The polymer extracted from the cells was analyzed by FTIR. The FTIR spectrum is provided in Fig. S1a. An absorption peak near 3290 cm^{-1} was detected which might be an indication of the stretching in the hydroxyl (O–H) group. Generally, the typical bond vibrations which suggest the presence of PHA is the ester carbonyl bond (C=O). These bond vibrations were observed near the region of $1720\text{--}1740 \text{ cm}^{-1}$. PHAs exhibit their characteristic band at 1719 cm^{-1} . Some other peaks were observed at 2914 cm^{-1} and 2879 cm^{-1} which could be accredited to CH_3 and CH_2 group stretching respectively. Other peaks in the range of $1450\text{--}1000 \text{ cm}^{-1}$ could be attributed to CH_3 bending, CH_2 wagging, C–O, C–C, and C–O–C stretching. The FTIR spectra analysis suggested that the extracted polymer was P(3HB-co-3HV) in nature. Instances in literature also suggest similar findings according to FTIR spectra (Alsafadi et al., 2020; Mahansaria et al., 2020; Steinbruch et al., 2020).

3.3.2. TGA/DSC thermal analyses

Thermal characteristics of PHA were estimated from the TGA thermogram (Fig. S1b). The temperature of decomposition minima (T_d) was observed to be $247.4 \text{ }^\circ\text{C}$. The thermogram also suggested a loss of weight $\sim 86.2\%$. The melting temperature of the PHA produced was estimated to be $175.8 \text{ }^\circ\text{C}$ from the DSC analysis.

3.3.3. ¹H NMR analysis

The chemical composition of the polymer was analyzed using ¹H NMR. The peaks obtained in the ¹H NMR spectrum could be attributed to individual carbon atoms in the monomers. Proton peaks at 0.83 and 1.26 ppm were attributed to the CH_3 group of 3HB and 3HV. Proton peaks of CH_2 for 3HV were observed at 1.57 and 2.58 ppm . For 3HB, the CH_2 proton peaks were observed at 2.48 ppm . The peaks for the CH group were observed at 5.25 ppm which suggested the presence of CH group for 3HB and 3HV (Fig. S2d). In order to determine the molar composition of the polymer repeating units, the area ratio of the methyl resonance peaks from 3HV unit ($\delta = 0.83$) and 3HB unit ($\delta = 1.26 \text{ ppm}$) was calculated from the ¹H NMR spectrum. Accordingly, the monomer compositions were calculated with a 3HB and 3HV composition of 90.4% and 10.6% respectively. Comparable explanations have

also been defined in earlier works for P(3HB-co-3HV) production (Alsafadi et al., 2020; Don et al., 2006).

3.4. GC/MS analysis

3.4.1. GC/MS analysis of the hydrolysates

The hydrolysate was analyzed using GC/MS to determine the various complex compounds obtained after hydrolysis (Fig. S2). All the components that were identified by GC/MS have been provided in the supplementary material. The obtained values were compared with a NIST database and major components of the hydrolysate were recognized. The major products identified were ketones such as 2-methyl 2-cyclopentenone followed by aldehydes and furfurals. Similar results for hydrolysate analysis were observed by Anastaskis and Ross (Anastaskis and Ross, 2011), in subcritical hydrolysis of the brown algae, *Laminaria saccharina*. It can be speculated that the ketones and phenols are degradation products of the complex carbohydrates and cellulose of the biomass. Similarly, proteins decompose to form nitrogen-rich compounds. Cyclopentenone was found to increase at higher temperatures whereas the quantities of 5-methyl furfural were not present at lower temperatures. This also corresponds to our observation by Taguchi optimization where higher temperatures corresponded to higher amounts of 5-HMF. This suggests that temperature is a key factor to determine the quality of seaweed hydrolysate for PHA production. Fatty acid fractions were not observed. This might be due to the low lipid content of macroalgal biomass which led to the conversion of fatty acids into various other products at different temperatures.

3.4.2. GC/MS analysis of the PHA produced

To determine the chemical composition of the polymer, GC/MS analysis was performed to analyze the butyl ester of PHA. Two peaks were observed in the chromatogram with retention times of 9.46 and 10.654 min. After comparison with the MS database, the peaks were identified as butyl esters of 3-hydroxybutyrate (3HB) and 3-hydroxy valerate (3HV) respectively. GC/MS analysis thus suggested that the PHA obtained after fermentation using *H. mediterranei* was composed of 3HB and 3HV

monomer units. Previous studies have also suggested similar polymer compositions for PHA production from *H. mediterranei* (Zhao et al., 2015).

3.5. Molecular weight analysis of PHA produced

Gel Permeation Chromatography (GPC) was utilized to determine the average molecular weights of the extracted PHA. The number average molecular weight (M_n) was observed to be 576 kDa using polystyrene (PS) standard and 584 kDa using polymethyl methacrylate (PMMA) standard. The average molecular weight (M_w) was found to be 963 kDa and 916 kDa for PS and PMMA standards respectively. The polydispersity index (PDI) is a measure of the homogeneity of the polymer. The PDI of extracted PHA was calculated to be 1.679 and 1.562 for PS and PMMA standards respectively. The observed values of molecular weight and PDI were similar to previously reported data for high-quality PHA production from *Haloferax mediterranei* (Alsafadi et al., 2020). For the polymer to be of varied usage, the average molecular weight should be high with a low heterogeneity (PDI in a range of 1.5–2.0) (Mahansaria et al., 2020). The values observed for our PHA extracted from *H. mediterranei* showed average molecular weights and PDI in the same range which suggested the quality of PHA produced.

3.6. Biochar yields from various Taguchi experiments

The solid residue yields were quantified for each Taguchi experimental level. The solid residue comprises biochar and water-soluble solids. Fig. 4 summarizes the solid mass recovery. The solid recovery is 71–85% of the initial biomass with biochar yields of 5–24%. The water-soluble solids include hydrolyzed carbohydrate fragments with different lengths, amino acids, and soluble ash. The rest of the mass can be accounted for released algae moisture, water produced due to the carbonization process, and liquids formed in the process. The highest biochar yield was $19.4 \pm 1.23\%$, the water-soluble solids yield is $58.2 \pm 0.45\%$, moisture that was released during the process comprised of $19.1 \pm 0.88\%$ and the rest ($3.3 \pm 0.13\%$) can be attributed to produced water and volatile liquids.

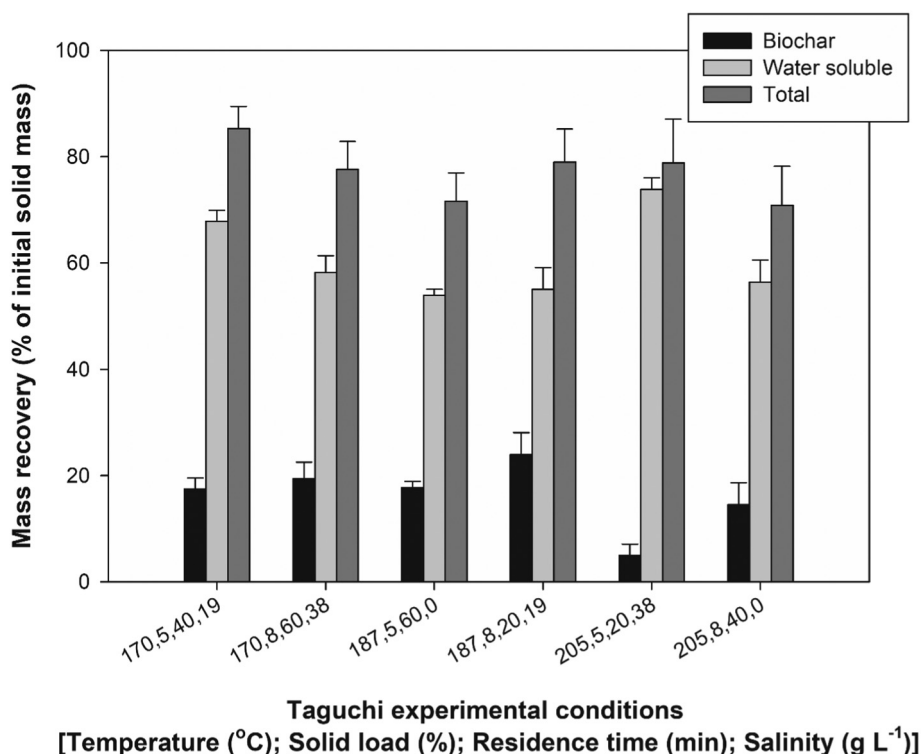


Fig. 4. Average solid residue mass recovery for various Taguchi experiments.

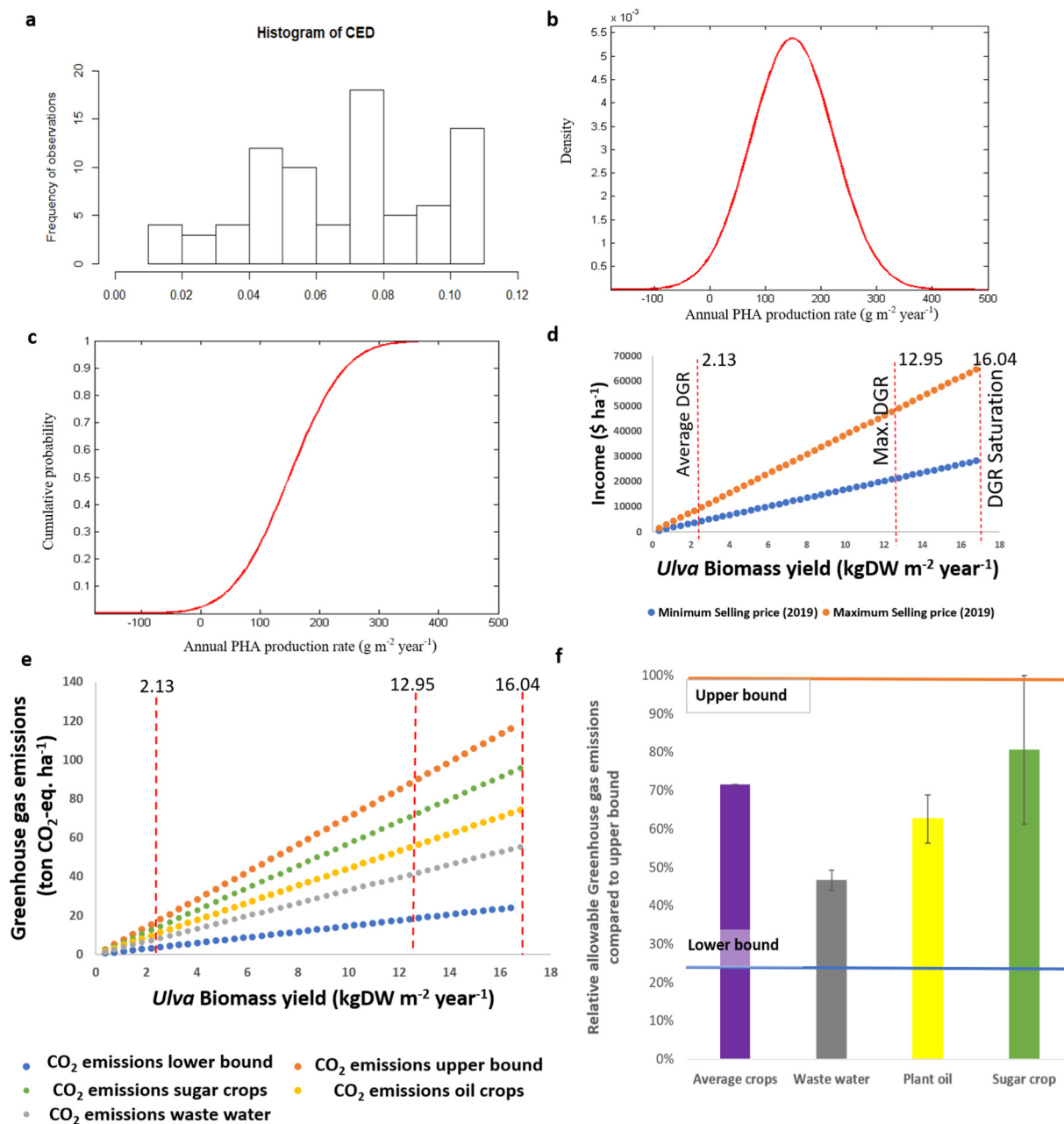


Fig. 5. Revenue estimation of PHA production from offshore-cultivated biomass. (a) Conversion efficiency distribution (CED) based on meta-data analysis of fermentation. (b) Annual PHA production rate (APPR) probability density function. (c) Annual PHA production rate (APPR) cumulative density function. (d) Estimated annual income from the production of PHA derived from offshore cultivated macroalgae. (e) Estimated allowable greenhouse gas emissions from the production of PHA derived from offshore cultivated macroalgae. (f) Relative allowable greenhouse gas emissions for various PHA substrates compared to upper bound (Maximum for feedstocks based on sugar crops). The Lower bound represents fossil HDPE emissions.

3.7. Preliminary revenue analysis for offshore derived biomass for PHA

The probability distribution of PHA production from biomass which was previously denoted as CED is shown in Fig. 5a. Fig. 5b and c show

the annual PHA production rate (APPR) and its cumulative distribution function respectively. The mean APPR of *Ulva* sp. cultivated under offshore conditions is $148.14 \text{ g PHA m}^{-2} \text{ year}^{-1}$. For a process to be feasible, it should be economically viable which is also true for PHA

Table 3

Sensitivity analysis of the income and required biomass costs with the *Ulva* biomass to PHA conversion efficiencies.

Confidence of APPR	99%	95%	90%	85%	80%
APPR ($\text{g PHA m}^{-2} \text{ year}^{-1}$)	142.09 ± 0.56	143.54 ± 0.63	148.14 ± 0.42	152.74 ± 0.38	154.19 ± 0.23
Low Income ($\$2.4 \text{ kg}^{-1}$ selling price) $\$ \text{ ha}^{-1}$	3410.16 ± 0.08	3444.96 ± 0.06	3555.36 ± 0.11	3665.76 ± 0.16	3700.56 ± 0.05
High Income ($\$5.5 \text{ kg}^{-1}$ selling price) $\$ \text{ ha}^{-1}$	7814.95 ± 0.07	7894.70 ± 0.09	8147.70 ± 0.12	8400.70 ± 0.14	8480.45 ± 0.03
$C_{DW_Biomass} \text{ } \$ \text{ ton}^{-1}$ (low)	11.21 ± 0.04	11.32 ± 0.06	11.68 ± 0.04	12.05 ± 0.06	12.16 ± 0.08
$C_{DW_Biomass} \text{ } \$ \text{ ton}^{-1}$ (high)	25.68 ± 0.06	25.95 ± 0.09	26.78 ± 0.08	27.61 ± 0.07	27.87 ± 0.09

Table 4

Sensitivity analysis of the allowable greenhouse gas emissions for PHA production from *Ulva* biomass. Lower bound = 'HDPE competitive', upper bound = 'highest reported crop PHA competitive'.

Confidence of APPR	99%	95%	90%	85%	80%
APPR (g PHA m ⁻² year ⁻¹)	142.09 ± 0.56	143.54 ± 0.63	148.14 ± 0.42	152.74 ± 0.38	154.19 ± 0.23
Total CO ₂ emissions, lower bound (ton ha ⁻¹ year ⁻¹)	2.97 ± 0.02	3.00 ± 0.05	3.10 ± 0.04	3.19 ± 0.03	3.22 ± 0.02
Total CO ₂ emissions, upper bound (ton ha ⁻¹ year ⁻¹)	14.35 ± 0.08	14.50 ± 0.06	14.96 ± 0.05	15.43 ± 0.07	15.57 ± 0.06
Allowable E _{DW_biomass} CO ₂ , lower bound (kg CO ₂ ton ⁻¹ seaweed ⁻¹)	9.76 ± 0.03	9.86 ± 0.02	10.18 ± 0.04	10.49 ± 0.03	10.59 ± 0.05
Allowable E _{DW_biomass} CO ₂ , upper bound (kg CO ₂ ton ⁻¹ seaweed ⁻¹)	47.16 ± 0.07	47.64 ± 0.11	49.17 ± 0.08	50.70 ± 0.12	51.18 ± 0.04

production. But for PHA production using seaweed, large offshore facilities for biomass production are unavailable currently. The information available in the literature about the economics of PHA production from seaweeds is scarce (Levett et al., 2016; Roesijadi et al., 2008). Studies have focussed mainly on the life cycle impact of food-derived plastics (PHA) as compared to polyethylene (PE) (Kim and Dale, 2005). Most of the companies producing PHA have rarely used inexpensive feedstocks let alone seaweeds for PHA production. The market prices of PHA vary between \$2.4 - \$5.5 kg⁻¹ (Crutchik et al., 2020). The current price of PHA is known and is not competitive with regular fossil plastics. The goal is to find a point when they will be. Utilizing the current market data, the PHA production from seaweed (*Ulva* sp.) cultivated in the Israeli coasts (APPR of 148.14 g PHA m⁻² year⁻¹) will incur an annual income of \$0.336 m⁻² year⁻¹ (\$3360 ha⁻¹ year⁻¹) to \$0.77 m⁻² year⁻¹ (\$7700 ha⁻¹ year⁻¹). The investment in seaweed farming and additional costs for biomass processing are also determined by these market prices. The maximum price of biomass production and processing can be estimated to maintain a breakeven with the current market prices and our average productivity (~5.8 gDW m⁻² d⁻¹ or 2125 gDW m⁻² year⁻¹) was found to be ~\$158- \$362ton⁻¹. If we assume that the cost of raw materials is 30% of the total costs of PHA production (Chemodanov et al., 2017), the maximum price of the biomass should be ~\$47 - \$108 ton⁻¹. The current price of seaweed production amount to an average of \$785 ton⁻¹ (Ferdouse et al., 2018; Steinbruch et al., 2020). A sensitivity analysis was also done to analyze the possible costs for biomass production and probable income from offshore cultivation compared to the observed conversion efficiencies. This was shown in Table 3.

Sensitivity analysis was performed to understand the potential income which could be obtained using the yields as observed in the present study. This is shown in Fig. 5d. The income has an increasing trend as we raise the productivity from average (5.8 gDW m⁻² day⁻¹) to the maximum productivity observed offshore (35.49 gDW m⁻² day⁻¹). This led to an increase in the income from \$612-\$1404 ha⁻¹ year⁻¹ to \$28,197-\$64,619 ha⁻¹ year⁻¹. A previous study on ethanol production from seaweeds estimated an enhanced potential income of \$8625-\$20,190 ha⁻¹ year⁻¹ (Chemodanov et al., 2017). The challenges for the commercialization of biobased plastics include high costs of production as well as competition for using arable land resources (Shen et al., 2010). The present process for PHA production using seaweed biomass could be much more economically beneficial to the farmer as compared to the production of bioethanol. The process could also provide a sustainable and economically viable method for bioplastic production. This intensification can only be possible if offshore technologies are developed along with onshore technologies available which remains a challenge for the biorefinery process (Bruhn et al., 2011; Golberg and Liberzon, 2015).

3.8. Allowable greenhouse gas emissions of offshore derived biomass for PHA

The state of the art biobased PHA GHG emissions depend on the feedstock and processing route (Narodoslawsky et al., 2015). State-of-the-art emissions for wastewater based PHA are estimated to be between 4.44 and 4.98 kg CO₂-equivalent kg⁻¹ PHA (no feedstock emissions) (Dacosta et al., 2015), sugar-based PHA between 6.18 and 10.10 kg CO₂-equivalent kg⁻¹ PHA (including mass-allocated feedstock

emissions) (Kookos et al., 2019), and oil crop-based PHA 5.68-6.96 kg CO₂-equivalent kg⁻¹ PHA (including mass-allocated feedstock emissions) (Kookos et al., 2019), all without biogenic CO₂ and co-product credits. Using these GHG emissions data, a priori the maximum allowable GHG emissions for the production of PHA from *Ulva* were derived. An APPR of 148.14 g PHA m⁻² year⁻¹ will lead to yearly allowable emissions of 0.29 kg CO₂-equivalent year⁻¹ (2926 kg CO₂-eq. ha⁻¹ year⁻¹,- scenario 'HDPE competitive' emissions) to 1.41 kg CO₂-equivalent year⁻¹ (14,140 kg CO₂-eq. ha⁻¹ year⁻¹, scenario 'highest reported crop PHA competitive' emissions). To maintain a break-even in terms of emissions using the average productivity (~5.8 gDW m⁻² day⁻¹ or 2125 gDW m⁻² year⁻¹), the maximum allowable emissions for production are then 138-665 kg CO₂-eq. ton⁻¹ seaweed. Assuming that feedstock production accounts for 35% of the emissions of biobased PHA (Akiyama et al., 2003), the maximum allowable emissions are reduced to 48-233 kg CO₂-eq. ton⁻¹ seaweed. Reported emissions range from 125 kg CO₂ eq ton⁻¹ seaweed (Alvarado-Morales et al., 2013) to 438 kg CO₂ eq ton⁻¹ seaweed (Brockmann et al., 2015). The latter was largely influenced by indirect emissions from nutrient consumption required for the onshore cultivation of seaweed. This indicates that efficient design of the cultivation infrastructure is essential to minimize emissions from material inputs and at the same time optimize biomass yields to achieve emissions in the order of magnitude of 48-233 kg CO₂ eq ton⁻¹ seaweed. Table 4 shows the sensitivity analysis and compares the results of allowable emissions from offshore cultivation facilities to the current scenarios.

The sensitivity analysis of GHG emissions as a function of observed yields in the present study appears in Fig. 5e. The relative allowable GHG emissions for various substrates are shown in Fig. 5f. The allowable GHG emissions for seaweed PHA have an increasing trend going hand-in-hand with increased productivity from the average daily growth rate until the maximum observed offshore productivity. At an average daily growth, the allowable emissions are 2.7-12.9 ton ha⁻¹, increasing to allowable emissions of 18.1-87.7 ton ha⁻¹ at maximum daily growth rates. These bounds indicate the operating window for seaweed, e.g. to be competitive to PHA production from wastewater the maximum allowable emissions are 46.6% ± 2.7% of the upper bound scenario (i.e. competitiveness to the highest crop PHA emissions). The very few reported GHG emissions for seaweed cultivation are 21.5 tons CO₂ eq. ha⁻¹ (Brockmann et al., 2015) and 59.4 ton CO₂ eq. ha⁻¹ (van Oirschot et al., 2017).

In the biorefinery process, the revenue generated from the biochar by-product should be considered as well. Considering the annual seaweed biomass production, the biochar yield amounted to 42.6 g m⁻² year⁻¹. Due to its higher calorific value (adjusted HHV of 17 MJ kg⁻¹) (Greiserman et al., 2019), the biochar obtained could be utilized for co-combustion in thermal power plants thus reducing the environmental burden. The breakeven market price for the production of biochar is estimated to be \$0.6 kg⁻¹ (\$600 ton⁻¹) (Yoder et al., 2011). Considering the yield of biochar from the proposed process (~20% w/w), the maximum revenue generated could amount to up to \$0.12 kg⁻¹ (\$120 ton⁻¹). Considering the annual yield of seaweed biomass, the maximum revenue generated from biochar can be estimated to up to \$8048 ha⁻¹ of cultivated area. Assuming that credits from biochar are based on the average of currently produced heat (0.119 kg CO₂ eq. MJ⁻¹ heat,) (Myhre, 2014), the total emissions could be reduced

with 0.405 kg CO₂ eq kg⁻¹ seaweed. Assuming that the maximum allowable emissions from biochar are based on future heat production (0.031 kg CO₂ eq MJ⁻¹ heat) (Myhre, 2014), the total emissions could be reduced with 0.106 kg CO₂ eq kg⁻¹ seaweed. This could be an added incentive for the biorefinery thereby increasing the revenue generated and decreasing the emissions from the process to a greater extent. The analysis (economic and greenhouse gas) presented in the present work provides an insight into the revenues generated from PHA production using macroalgal biomass and the preliminary emissions associated with the process. In depth analysis of the process requires an extensive techno-economic analysis and LCA assessment to assess the performance of the system.

4. Conclusions

The present study evaluated the intensification of process parameters for the simultaneous production of PHA and biochar from seaweed biomass. Taguchi method optimization suggested the important factors which could determine the PHA productivity. GC/MS and molecular weight analysis of the PHA provided an insight into the quality of the polymer. A preliminary economic analysis suggested that for the process to be economically feasible, the biomass should be provided for \$47–\$108 ton⁻¹. Estimation of greenhouse gases proposed that efficient design of the cultivation infrastructure is essential to minimize emissions and at the same time optimize biomass yields.

CRedit authorship contribution statement

Supratim Ghosh: Investigation, Data curation, Formal analysis, Writing – review & editing. **Semion Greiserman:** Investigation, Writing – review & editing. **Alexander Chemodanov:** Investigation, Writing – review & editing. **Petronella Margaretha Slegers:** Investigation, Data curation, Writing – review & editing. **Bogdan Belgorodsky:** Investigation, Writing – review & editing. **Michael Epstein:** Investigation, Writing – review & editing. **Abraham Kribus:** Investigation, Writing – review & editing. **Michael Gozin:** Investigation, Writing – review & editing. **Guo-Qiang Chen:** Investigation, Writing – review & editing. **Alexander Golberg:** Conceptualization, Methodology, Writing – original draft.

Declaration of competing interest

The authors declare that they have no known competing financial interests or personal relationships that could have appeared to influence the work reported in this paper.

Acknowledgments

The authors thank TAU XIN Centre and The Aaron Frenkel Air Pollution Initiative at Tel Aviv University for financial support.

Appendix A. Supplementary data

Supplementary data to this article can be found online at <https://doi.org/10.1016/j.scitotenv.2021.145281>.

References

- Abdallah, M. Ben, Karray, F., Sayadi, S., 2020. Production of polyhydroxyalkanoates by two halophilic archaeal isolates from Chott El Jerid using inexpensive carbon sources. *Biomolecules* 10. <https://doi.org/10.3390/biom10010109>.
- Akiyama, M., Tsuge, T., Doi, Y., 2003. Environmental life cycle comparison of polyhydroxyalkanoates produced from renewable carbon resources by bacterial fermentation. *Polym. Degrad. Stab.* 80, 183–194. [https://doi.org/10.1016/S0141-3910\(02\)00400-7](https://doi.org/10.1016/S0141-3910(02)00400-7).
- Allers, T., Barak, S., Liddell, S., Wardell, K., Mevarech, M., 2010. Improved strains and plasmid vectors for conditional overexpression of His-tagged proteins in *Haloflex*

- volcanii*. *Appl. Environ. Microbiol.* 76, 1759–1769. <https://doi.org/10.1128/AEM.02670-09>.
- Alsafadi, D., Ibrahim, M.I., Alamry, K.A., Hussein, M.A., Mansour, A., 2020. Utilizing the crop waste of date palm fruit to biosynthesize polyhydroxyalkanoate bioplastics with favorable properties. *Sci. Total Environ.* 737, 139716. <https://doi.org/10.1016/j.scitotenv.2020.139716>.
- Alvarado-Morales, M., Boldrin, A., Karakashev, D.B., Holdt, S.L., Angelidaki, I., Astrup, T., 2013. Life cycle assessment of biofuel production from brown seaweed in Nordic conditions. *Bioresour. Technol.* 129, 92–99. <https://doi.org/10.1016/j.biortech.2012.11.029>.
- Anastasakis, K., Ross, A.B., 2011. Hydrothermal liquefaction of the brown macro-alga *Laminaria Saccharina*: effect of reaction conditions on product distribution and composition. *Bioresour. Technol.* 102, 4876–4883. <https://doi.org/10.1016/j.biortech.2011.01.031>.
- Arumugam, A., Yogalaksha, P., Furhanashereen, M., Ponnusami, V., 2020. Statistical optimization and enhanced synthesis of polyhydroxyalkanoates from *Ceiba pendantra* oil as novel non-edible feedstock. *Biomass Convers. Biorefinery*. <https://doi.org/10.1007/s13399-020-00742-w>.
- Brockmann, D., Pradinaud, C., Champenois, J., Benoit, M., Hélias, A., 2015. Environmental assessment of bioethanol from onshore grown green seaweed. *Biofuels. Bioprod. Biorefining* 9, 696–708.
- Brown, A.E., Finnerty, G.L., Camargo-Valero, M.A., Ross, A.B., 2020. Valorisation of macroalgae via the integration of hydrothermal carbonisation and anaerobic digestion. *Bioresour. Technol.* 312, 123539. <https://doi.org/10.1016/j.biortech.2020.123539>.
- Bruhn, A., Dahl, J., Nielsen, H.B., Nikolaisen, L., Rasmussen, M.B., Markager, S., Olesen, B., Arias, C., Jensen, P.D., 2011. Bioenergy potential of *Ulva lactuca*: biomass yield, methane production and combustion. *Bioresour. Technol.* 102, 2595–2604. <https://doi.org/10.1016/j.biortech.2010.10.010>.
- Cesário, M.T., da Fonseca, M.M.R., Marques, M.M., de Almeida, M.C.M.D., 2018. Marine algal carbohydrates as carbon sources for the production of biochemicals and biomaterials. *Biotechnol. Adv.* 36, 798–817. <https://doi.org/10.1016/j.biotechadv.2018.02.006>.
- Chemodanov, A., Jinjikhshvily, G., Habiby, O., Liberzon, A., Israel, A., Yakhini, Z., Golberg, A., 2017. Net primary productivity, biofuel production and CO₂ emissions reduction potential of *Ulva* sp. (*Chlorophyta*) biomass in a coastal area of the Eastern Mediterranean. *Energy Convers. Manag.* 148, 1497–1507. <https://doi.org/10.1016/j.enconman.2017.06.066>.
- Crutchik, D., Franchi, O., Caminos, L., Jeison, D., Belmonte, M., Pedrouso, A., Val del Rio, A., Mosquera-Corral, A., Campos, J.L., 2020. Polyhydroxyalkanoates (PHAs) production: a feasible economic option for the treatment of sewage sludge in municipal wastewater treatment plants? *Water (Switzerland)* 12, 1–12. <https://doi.org/10.3390/W12041118>.
- Cui, J., Shi, J., Zhang, J., Wang, L., Fan, S., Xu, Z., Huo, Y., Zhou, Q., Lu, Y., He, P., 2018. Rapid expansion of *Ulva* blooms in the Yellow Sea, China through sexual reproduction and vegetative growth. *Mar. Pollut. Bull.* 130, 223–228. <https://doi.org/10.1016/j.marpolbul.2018.03.036>.
- Dacosta, C.F., Posada, J.A., Ramirez, A., 2015. Large scale production of Polyhydroxyalkanoates (PHAs) from wastewater: a study of techno-economics, energy use and greenhouse gas emissions. *Int. J. Environ. Chem. Ecol. Geophys. Eng.* 9, 433–438.
- Don, T.M., Chen, C.W., Chan, T.H., 2006. Preparation and characterization of poly (hydroxyalkanoate) from the fermentation of *Haloflex mediterranei*. *J. Biomater. Sci. Polym. Ed.* 17, 1425–1438. <https://doi.org/10.1163/156856206778937208>.
- Ferdouse, F., Løvstad Holdt, S., Smith, R., Murúa, P., Yang, Z., 2018. The global status of seaweed production, trade and utilization. *FAO Globefish Res. Program.* 124, 120.
- Gao, G., Clare, A.S., Rose, C., Caldwell, G.S., 2018. *Ulva rigida* in the future ocean: potential for carbon capture, bioremediation and biomethane production. *GCB Bioenergy* 10, 39–51. <https://doi.org/10.1111/gcbb.12465>.
- Gao, G., Wu, M., Fu, Q., Li, X., Xu, J., 2019. A two-stage model with nitrogen and silicon limitation enhances lipid productivity and biodiesel features of the marine bloom-forming diatom *Skeletonema costatum*. *Bioresour. Technol.* 289, 121717.
- Gao, G., Burgess, J.C., Wu, M., Wang, S., Gao, K., 2020. Using macroalgae as biofuel: current opportunities and challenges. *Bot. Mar.* 1.
- Ghosh, S., Gnaïm, R., Greiserman, S., Fadeev, L., Gozin, M., Golberg, A., 2019. Macroalgal biomass subcritical hydrolysates for the production of polyhydroxyalkanoate (PHA) by *Haloflex mediterranei*. *Bioresour. Technol.* 271, 166–173. <https://doi.org/10.1016/j.biortech.2018.09.108>.
- Golberg, A., Liberzon, A., 2015. Modeling of smart mixing regimes to improve marine biorefinery productivity and energy efficiency. *Algal Res.* 11, 28–32. <https://doi.org/10.1016/j.algal.2015.05.021>.
- Golberg, A., Zollmann, M., Prabhu, M., Palatnik, R.R., 2020. Enabling bioeconomy with offshore macroalgae biorefineries, in: *Bioeconomy for Sustainable Development*. Springer, pp. 173–200.
- Greetham, D., Adams, J.M., Du, C., 2020. The utilization of seawater for the hydrolysis of macroalgae and subsequent bioethanol fermentation. *Sci. Rep.* <https://doi.org/10.1038/s41598-020-66610-9>.
- Greiserman, S., Epstein, M., Chemodanov, A., Steinbruch, E., Prabhu, M., Guttman, L., Jinjikhshvily, G., Shamis, O., Gozin, M., Kribus, A., 2019. Co-production of monosaccharides and hydrochar from green macroalgae *Ulva* (*Chlorophyta*) sp. with subcritical hydrolysis and carbonization. *BioEnergy Res.* 12, 1090–1103.
- Hori, C., Yamazaki, T., Ribordy, G., Takisawa, K., Matsumoto, K., Ooi, T., Zinn, M., Taguchi, S., 2019. High-cell density culture of poly(lactate-co-3-hydroxybutyrate)-producing *Escherichia coli* by using glucose/xylose-switching fed-batch jar fermentation. *J. Biosci. Bioeng.* 127, 721–725. <https://doi.org/10.1016/j.jbiosc.2018.11.006>.
- Ibrahim, M.H.A., Steinbüchel, A., 2009. Poly(3-hydroxybutyrate) production from glycerol by *Zobellella denitrificans* MW1 via high-cell-density fed-batch fermentation and simplified solvent extraction. *Appl. Environ. Microbiol.* 75, 6222–6231. <https://doi.org/10.1128/AEM.01162-09>.

- Jayakody, L.N., Johnson, C.W., Whitham, J.M., Giannone, R.J., Black, B.A., Cleveland, N.S., Klingeman, D.M., Michener, W.E., Olstad, J.L., Vardon, D.R., Brown, R.C., Brown, S.D., Hettich, R.L., Guss, A.M., Beckham, G.T., 2018. Thermochemical wastewater valorization: via enhanced microbial toxicity tolerance. *Energy Environ. Sci.* 11, 1625–1638. <https://doi.org/10.1039/c8ee00460a>.
- Jones, E.S., Raikova, S., Ebrahim, S., Parsons, S., Allen, M.J., Chuck, C.J., 2020. Saltwater based fractionation and valorisation of macroalgae. *J. Chem. Technol. Biotechnol.* 95, 2098–2109. <https://doi.org/10.1002/jctb.6443>.
- Kim, S., Dale, B.E., 2005. Life cycle assessment study of biopolymers (Polyhydroxyalkanoates) derived from no-tilled corn. *Int. J. Life Cycle Assess.* 10, 200–210. <https://doi.org/10.1065/lca2004.08.171>.
- Kookos, I.K., Koutinas, A., Vlysidis, A., 2019. Life cycle assessment of bioprocessing schemes for poly(3-hydroxybutyrate) production using soybean oil and sucrose as carbon sources. *Resour. Conserv. Recycl.* 141, 317–328. <https://doi.org/10.1016/j.resconrec.2018.10.025>.
- Korzen, L., Pulidindi, I.N., Israel, A., Abelson, A., Gedanken, A., 2015. Single step production of bioethanol from the seaweed *Ulva rigida* using sonication. *RSC Adv.* 5, 16223–16229. <https://doi.org/10.1039/c4ra14880k>.
- Levett, I., Birkett, G., Davies, N., Bell, A., Langford, A., Laycock, B., Lant, P., Pratt, S., 2016. Techno-economic assessment of poly-3-hydroxybutyrate (PHB) production from methane - the case for thermophilic bioprocessing. *J. Environ. Chem. Eng.* 4, 3724–3733. <https://doi.org/10.1016/j.jece.2016.07.033>.
- Luong, Mulchandani, A., 1989. Microbial inhibition kinetics revisited. *Enzym. Microb. Technol.* 11, 66–73.
- Mahansaria, R., Dhara, A., Saha, A., Haldar, S., Mukherjee, J., 2018. Production enhancement and characterization of the polyhydroxyalkanoate produced by *Natrinema ajinwuenis* (as synonym) = *Natrinema altunense* strain RM-G10. *Int. J. Biol. Macromol.* 107, 1480–1490. <https://doi.org/10.1016/j.ijbiomac.2017.10.009>.
- Mahansaria, R., Bhowmik, S., Dhara, A., Saha, A., Mandal, M.K., Ghosh, R., Mukherjee, J., 2020. Production enhancement of poly(3-hydroxybutyrate-co-3-hydroxyvalerate) in Halogetometricum borinquense, characterization of the bioplastic and desalination of the bioreactor effluent. *Process Biochem.* 94, 243–257. <https://doi.org/10.1016/j.procbio.2020.04.004>.
- Mohd Zain, N.F., Paramasivam, M., Tan, J.S., Lim, V., Lee, C.K., 2020. Response surface methodology optimization of polyhydroxyalkanoate production by *Burkholderia cepacia* BPT1213 using waste glycerol from palm oil-based biodiesel production. *Biotechnol. Prog.* <https://doi.org/10.1002/btpr.3077>.
- Myhre, G.D., 2014. Anthropogenic and Natural Radiative Forcing, in: Intergovernmental Panel on Climate Change (Ed.), *Climate Change 2013 – The Physical Science Basis: Working Group I Contribution to the Fifth Assessment Report of the Intergovernmental Panel on Climate Change*. Cambridge University Press, Cambridge, pp. 659–740. doi:DOI: 10.1017/CBO9781107415324.018.
- Narodoslawsky, M., Shazad, K., Kollmann, R., Schnitzer, H., 2015. LCA of PHA production - Identifying the ecological potential of bio-plastic. *Chem. Biochem. Eng. Q.* 29, 299–305. doi:10.15255/CABEQ.2014.2262.
- van Oirschot, R., Thomas, J.B.E., Gröndahl, F., Fortuin, K.P.J., Brandenburg, W., Potting, J., 2017. Explorative environmental life cycle assessment for system design of seaweed cultivation and drying. *Algal Res.* 27, 43–54. <https://doi.org/10.1016/j.algal.2017.07.025>.
- Pacholak, A., Gao, Z.-L., Gong, X.-Y., Kaczorek, E., Cui, Y.-W., 2020. The metabolic pathways of polyhydroxyalkanoates and exopolysaccharides synthesized by *Haloferax mediterranei* in response to elevated salinity. *J. Proteome* 232, 104065. <https://doi.org/10.1016/j.jprot.2020.104065>.
- Pezoa-Conte, R., Leyton, A., Anugwon, I., von Schoultz, S., Paranko, J., Mäki-Arvela, P., Willför, S., Muszyński, M., Nowicki, J., Lienqueo, M.E., Mikkola, J.P., 2015. Deconstruction of the green alga *Ulva rigida* in ionic liquids: closing the mass balance. *Algal Res.* 12, 262–273. <https://doi.org/10.1016/j.algal.2015.09.011>.
- Polikovskiy, M., Gillis, A., Steinbruch, E., Robin, A., Epstein, M., Kribus, A., Golberg, A., 2020. Biorefinery for the co-production of protein, hydrochar and additional co-products from a green seaweed *Ulva* sp. with subcritical water hydrolysis. *Energy Convers. Manag.* 225, 113380. doi:10.1016/j.enconman.2020.113380.
- Prabhu, M.S., Israel, A., Palatnik, R.R., Zilberman, D., Golberg, A., 2020. Integrated biorefinery process for sustainable fractionation of *Ulva ohnoi* (Chlorophyta): process optimization and revenue analysis. *J. Appl. Phycol.* <https://doi.org/10.1007/s10811-020-02044-0>.
- Qarri, A., Israel, A., 2020. Seasonal biomass production, fermentable saccharification and potential ethanol yields in the marine macroalga *Ulva* sp. (Chlorophyta). *Renew. Energy* 145, 2101–2107. <https://doi.org/10.1016/j.renene.2019.07.155>.
- Rao, R.S., Kumar, C.G., Prakasham, R.S., Hobbs, P.J., 2008. The Taguchi methodology as a statistical tool for biotechnological applications: a critical appraisal. *Biotechnol. J.* <https://doi.org/10.1002/biot.200700201>.
- Robin, A., Kazir, M., Sack, M., Israel, A., Frey, W., Mueller, G., Livnev, Y.D., Golberg, A., 2018. Functional protein concentrates extracted from the green marine macroalga *Ulva* sp., by high voltage pulsed electric fields and mechanical press. *ACS Sustain. Chem. Eng.* 6, 13696–13705. <https://doi.org/10.1021/acssuschemeng.8b01089>.
- Roesijadi, G., Copping, A.E.E., Huesemann, M.H.H., Forster, J., Benemann, J.R., Thom, R.M., 2008. *Techno-Economic Feasibility Analysis of Offshore Seaweed Farming for Bioenergy and Biobased Products - Independent Research and Development Report - IR Number : PNWD-3931 - Battelle Pacific Northwest Division 115*.
- Ruiz, A., Rodn, R.M., Fernandes, B.D., Vicente, A., Teixeira, A., 2013. Hydrothermal processing, as an alternative for upgrading agriculture residues and marine biomass according to the biorefinery concept : A review 21, 35–51. doi:10.1016/j.rser.2012.11.069.
- Shen, L., Worrell, E., Patel, M., 2010. Present and future development in plastics from biomass. *Biofuels, Bioprod. Biorefining Innov. a Sustain. Econ.* 4, 25–40.
- Spiekermann, P., Rehm, B.H.A., Kalscheuer, R., Baumeister, D., Steinbüchel, A., 1999. A sensitive, viable-colony staining method using Nile red for direct screening of bacteria that accumulate polyhydroxyalkanoic acids and other lipid storage compounds. *Arch. Microbiol.* 171, 73–80. <https://doi.org/10.1007/s002030050681>.
- Steinbruch, E., Drabik, D., Epstein, M., Ghosh, S., Prabhu, M.S., Gozin, M., Kribus, A., Golberg, A., 2020. Hydrothermal processing of a green seaweed *Ulva* sp. for the production of monosaccharides, polyhydroxyalkanoates, and hydrochar. *Bioresour. Technol.* 318, 124263. doi:10.1016/j.biortech.2020.124263.
- Thompson, T.M., Young, B.R., Baroutian, S., 2019. Advances in the pretreatment of brown macroalgae for biogas production. *Fuel Process. Technol.* 195, 106151. <https://doi.org/10.1016/j.fuproc.2019.106151>.
- Vandi, L.J., Chan, C.M., Werker, A., Richardson, D., Laycock, B., Pratt, S., 2018. Wood-PHA composites: mapping opportunities. *Polymers (Basel)*. 10, 1–15. <https://doi.org/10.3390/polym10070751>.
- Venkata Mohan, S., Venkateswar Reddy, M., 2013. Optimization of critical factors to enhance polyhydroxyalkanoates (PHA) synthesis by mixed culture using Taguchi design of experimental methodology. *Bioresour. Technol.* 128, 409–416. <https://doi.org/10.1016/j.biortech.2012.10.037>.
- Xu, J., Li, C., Dai, L., Xu, C., Zhong, Y., Yu, F., Si, C., 2020. Biomass fractionation and lignin fractionation towards lignin valorization. *ChemSusChem* 13, 4284–4295. <https://doi.org/10.1002/cssc.202001491>.
- Yoder, J., Galinato, S., Granatstein, D., Garcia-Pérez, M., 2011. Economic tradeoff between biochar and bio-oil production via pyrolysis. *Biomass Bioenergy* 35, 1851–1862. <https://doi.org/10.1016/j.biombioe.2011.01.026>.
- Yoganandham, S.T., Sathyamoorthy, G., Renuka, R.R., 2020. Chapter 8 - Emerging extraction techniques: Hydrothermal processing, in: Torres, M.D., Kraan, S., Dominguez, H.B.T.-S.S.T. (Eds.), *Advances in Green Chemistry*. Elsevier, pp. 191–205. doi:doi:10.1016/B978-0-12-817943-7.00007-X.
- Yu, K.L., Chen, W.H., Sheen, H.K., Chang, J.S., Lin, C.S., Ong, H.C., Show, P.L., Ng, E.P., Ling, T.C., 2020. Production of microalgal biochar and reducing sugar using wet torrefaction with microwave-assisted heating and acid hydrolysis pretreatment. *Renew. Energy* 156, 349–360. <https://doi.org/10.1016/j.renene.2020.04.064>.
- Zhao, Y.X., Rao, Z.M., Xue, Y.F., Gong, P., Ji, Y.Z., Ma, Y.H., 2015. Poly(3-hydroxybutyrate-co-3-hydroxyvalerate) production by Haloarchaeon *Haloferax mediterranei*. *Appl. Microbiol. Biotechnol.* 99, 7639–7649. <https://doi.org/10.1007/s00253-015-6609-y>.